Available online at www.sciencedirect.com
ScienceDirect
Journal of Power Sources 175 (2008) 669–674
JOURNAL OF POWER SOURCES
www.elsevier.com/locate/jpowsour

Short communication

Cathodic deposition and characterization of tin oxide coatings on graphite for electrochemical supercapacitors

Mengqiang Wu [a,*], Liping Zhang [b], Dongmei Wang [a], Chao Xiao [a], Shuren Zhang [a]

[a] *State Key Laboratory of Electronic Thin Films and Integrated Devices, School of Microelectronics and Solid State Electronics, University of Electronic Science and Technology of China, Chengdu 610054, PR China*
[b] *Department of Materials and Chemical Engineering, Sichuan University of Science and Engineering, No.180, Xueyuan Street, Huixing Road, Zigong 643000, PR China*

Received 15 June 2007; received in revised form 15 September 2007; accepted 19 September 2007
Available online 29 September 2007

Abstract

Amorphous tin oxide (SnO_x) was cathodically deposited onto graphite electrode in a bath containing 0.1 M stannous chloride ($SnCl_2$), 0.5 M sodium nitrate ($NaNO_3$), and 0.4 M nitric acid (HNO_3) in an aqueous solution of 50% (v/v) ethanol. The SnO_x coatings grown on graphite were characterized as typical capacitive behaviors by cyclic voltammetry (CV), chronopotentiometric (CP) in 0.5 M KCl. Specific capacitance (in millifarad per square centimeter, C_a) changes linearly with the deposition charge up to 4.5 C cm^{-2}, and a maximum of as high as 355 mF cm^{-2} was obtained with the SnO_x coating grown at around 5 C cm^{-2}. For the SnO_x coating deposited at 0.2 C cm^{-2}, a maximum specific capacitance (in farad per gram, C_m) of 298 and 125 F g^{-1} was achieved from CVs at a scan rate of 10, and 200 mV s^{-1}, respectively. The value of C_m significantly gets lower from 265 to around 95 F g^{-1} when the deposition charge increases from 0.2 to around 6.0 C cm^{-2}. The long cycle-life and stability of the SnO_x coatings on graphite via the presented cathodic deposition were also demonstrated.

Keywords: Tin oxide; Coatings; Cathodic deposition; Electrochemical capacitors; Supercapacitors

1. Introduction

In recent decades, electrochemical supercapacitors with high specific power and energy have been attracting considerable attention. Besides highly porous materials (e.g., activated carbon) with very high specific surface area, the electro-active materials transition such as metal oxides [1–18], nitrides [20,21] and conducting polymers [22–24] and their composites [25–27] with reversible redox transitions between various oxidation states are considered to be promising materials for the applications of redox supercapacitors. Among the capacitive oxides, the noble metal oxides such as amorphous phase of ruthenium oxide [1,2] and iridium oxide [3], have been demonstrated as high performance electro-active materials for redox supercapacitors. Most significantly, amorphous hydrous ruthenium oxide (a-$RuO_2{\cdot}nH_2O$) performs excellent pseudo-capacitive behaviors with specific capacitance as large as approaching 10^3 F g^{-1} and great reversibility, but the lack of abundance and high cost of the precious metal are the major disadvantages for commercial applications. More effort has been accordingly directed to alternative inexpensive electro-active materials for pseudo-capacitors such as nickel oxide [4–9], cobalt oxide [10–12], manganese oxide [13–15], vanadium oxide [16,17], and magnetite [18,19].

Most interestingly, as for its nontoxicity and abundant presence in nature, tin oxide (SnO_2) as anodes in lithium-ion batteries have been studied [28]. In the previous application of SnO_2 for supercapacitors, an Sb-doped SnO_2 nanocrystallites derived from a sol–gel process was examined in 1 M KOH electrolyte [29]. SnO_2 was also used as a dopant into RuO_2 for supercapacitors. A composite supercapacitor containing SnO_2 and electroplated RuO_2 was reported by Kuo and Wu [30]. Kim et al. [31] investigated RuO_2–SnO_2 nanocrystalline-embedded amorphous electrode for thin film microsupercapacitors. Nanostructured SnO_2–Al_2O_3 were synthesized for supercapacitor application in 0.1 M NaCl solutions, giving a supercapacitance

* Corresponding author. Tel.: +86 28 83207920; fax: +86 28 83202139.
E-mail address: mwu@uestc.edu.cn (M. Wu).

0378-7753/$ – see front matter © 2007 Elsevier B.V. All rights reserved.
doi:10.1016/j.jpowsour.2007.09.062

of 119 F g^{-1} [32]. Prasad and Miura [33] employed potentiodynamical electrodeposition to SnO_2 for supercapacitor applications in 0.1 M Na_2SO_4, achieving supercapacitance as high as 285 and 101 F g^{-1} at a scan rate of 10 and 200 mV s^{-1}, respectively. In addition, Rao et al. [34] recognized nano-sized SnO as a promising electrode material for electrochemical capacitors.

In the present work, amorphous nanostructured tin oxide (SnO_x) coatings were grown onto graphite disc electrodes at room temperature by cathodic electrodeposition from an aqueous medium of stannous chloride, and characterized as a supercapacitor electrode in neutral aqueous KCl electrolyte.

2. Experimental

Graphite disc electrodes (6 mm in diameter) were prepared in a procedure described elsewhere in detail [15]. The electrochemical cell for deposition was a three-electrode cell, in which a graphite disc was used as the working electrode, a platinum gauge as the counter electrode, and an Ag/AgCl (3 M KCl) electrode as the reference, respectively. Before deposition, oxygen was bubbled for 30 min in a bath containing 0.1 M stannous chloride ($SnCl_2$), 0.5 M sodium nitrate ($NaNO_3$), and 0.4 M nitric acid (HNO_3) in an aqueous solution of 50% (v/v) ethanol to allow stannous ions oxidized to stannic ions. It was observed that galvanostatic depositions might become unstable at higher currents with significant potential swings producing uncontrollable experimental conditions. A current density of 2.5 mA cm^{-2} was, thus, deliberately applied for specified time to achieve desired deposition charge on a CHI760B computer-controlled electrochemical workstation. Upon deposition, the coatings were rinsed with, and cleaned ultrasonically for 10 min in distilled water to remove the attached chloride ions. After being immersed in boiling water for 10 min, the coatings were dried by a flow of cool air.

The surface morphology of the SnO_x coatings was estimated on a JEOL JSM-5800LV scanning electron microscope (SEM). The thickness of the coatings was evaluated via SEM cross-sectional observations. In order to prepare a sample for an observation, a part of the electrode attached with the coating was cut off, and the epoxy sheath was removed to reveal the side view of the coating. The X-ray diffraction (XRD) measurements were carried out by means of an X-ray diffractometer (X'PertProMPD, Philips Co.). The energy dispersive X-ray analyses (EDX) data were collected on a JEOL JSM-6490LV scanning electron microscope (SEM).

The as-obtained electrodes were evaluated in an aqueous solution of 0.5 M KCl via cyclic voltammetry (CV) and chronopotentiometric (CP) on a model CHI760B electrochemical workstation. The average specific capacitance data were derived from both cyclic voltammetric currents and the charge–discharge measurements, which were normalised and compared in terms of the simple geometric area of the original graphite electrode surface. Attempts to weigh the mass of the SnO_x coatings on the electrode were not successful, due to the relatively large mass of the graphite disc electrode used. The mass of the SnO_x coatings was, however, determined by dissolving the coating in an H_2O_2/HNO_3 mixture and using an AA 6800 atomic absorption spectrometer (Shimadzu, Japan) flame atomic absorption spectrometry. All of the electrochemical measurements were carried out at room temperature in a three-electrode, single compartment cell with an Ag/AgCl (3 M KCl) reference electrode and a Pt wire counter electrode.

3. Results and discussion

A typical micrograph of the as-grown coating at 3.0 C cm^{-2} is shown in Fig. 1a and b obtained at a higher magnification. It can be seen clearly that the coating is uniformly deposited onto the surface of the graphite electrode. The deposit shows a nature of rough, porous and nanostructured morphology with many tiny nanowires. To identify the as-formed coating, XRD patterns were in addition recorded (not shown herein), positively indicating an amorphism. Nanocrystalline tin oxide coatings were, however, obtained by electrodeposition at 85 °C in nitric acid solution [35]. Therefore, without further heat-treatment, the coatings grown at room temperature were presumably the amorphous SnO_x. Thin films of nickel hydroxide were deposited electrochemically onto gold substrate in nitrate solutions, and porous nickel oxide films were consequently obtained via heat-treatment for electrochemical supercapacitors [36,37]. Similarly, we investigated the impacts of the substrate on the capacitive characteristics of nickel oxide film via the discussed cathodic deposition [38].

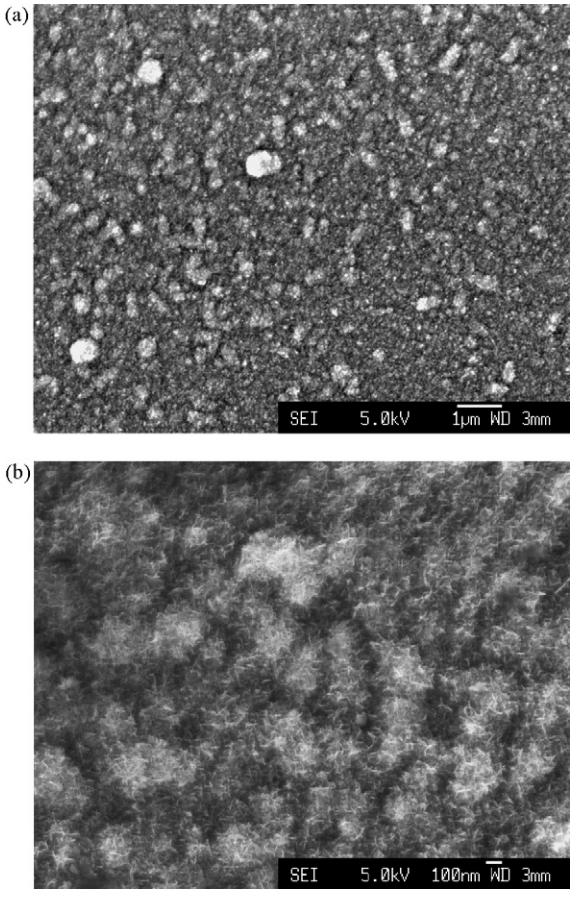

Fig. 1. SEM images of the surface of the as-grown SnO_x coating at 3.0 C cm^{-2}; (b) is at a higher magnification of (a).

As for a reasonable explanation as to how the amorphous SnO_x coatings were deposited onto graphite substrates, a possible way could be suggested as follows,

$$NO_3^- + H_2O + 8e \rightarrow NH_4^+ + 10OH^- \quad (1)$$

$$Sn^{2x+} + 2xOH^- \rightarrow Sn(OH)_{2x} \rightarrow SnO_x + xH_2O \quad (2)$$

On the cathode electrode surface, reaction (1) takes place to cause the formation of OH^- ions. The OH^- ions react with Sn^{2x+} ions from the solution to form tin hydroxide on the cathode surface, which is thereby converted readily to oxide, especially while assisted by extra immersion in boiling water. Actually, tin hydroxide was unstable with respect to tin oxide and highly irreversible dehydration was favored [39]. $2x$ is the average valence of the metal ions. Considering the presence of stannous ions in the solution, the value of x could not be equal to 2 exactly. EDX analyses indicated that if oxygen was bubbled effectively to allow stannous ions oxidized thoroughly to stannic ions, the as-grown were definitely SnO_2 coatings.

As shown in Fig. 2, it is found that the coating thickness increases as the deposition charge increases. A maximum thickness of 1.2 μm was achieved at a deposition charge of around 5.5 C cm^{-2}. The attempted deposition at a deposition charge of above this value may cause the coating peeled off from the substrate and no further deposition was observed. This could be ascribed to the tensile stress leading to delamination when the coating becomes thick. The deposition rate nearly maintains a constant within 4.5 C cm^{-2}, and then decreases gradually. The decrease of deposition rate might be attributed to significant increase of the resistance of the deposit. Most significantly, as shown in Fig. 2b, the mass of coating exhibits a nice linearity with deposition charge, implying a coulombic efficiency of around 752 μg C^{-1}. Extreme care, however, had to be taken with relatively thick coatings. Small pieces inevitably peeled off the coating especially when changing the electrochemical solution for measurements of the electrochemical capacitance.

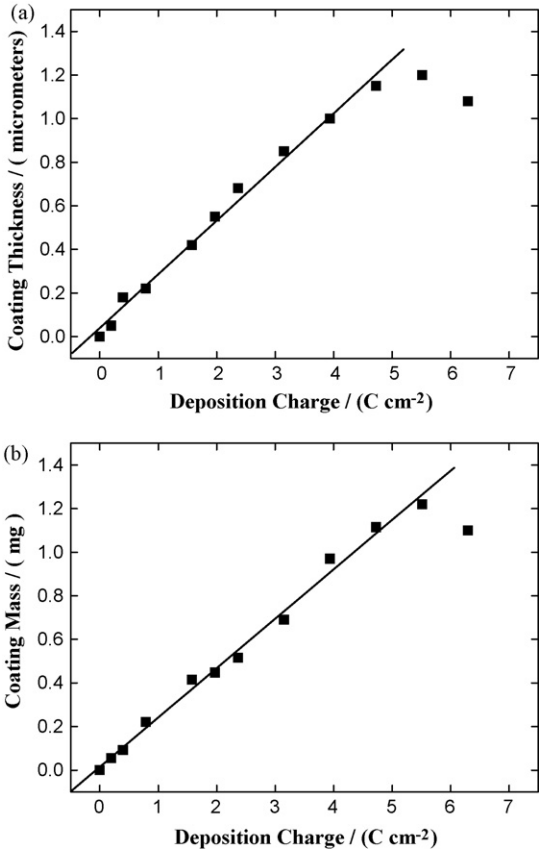

Fig. 2. Variation of coating thickness (a) and mass (b) with deposition charge.

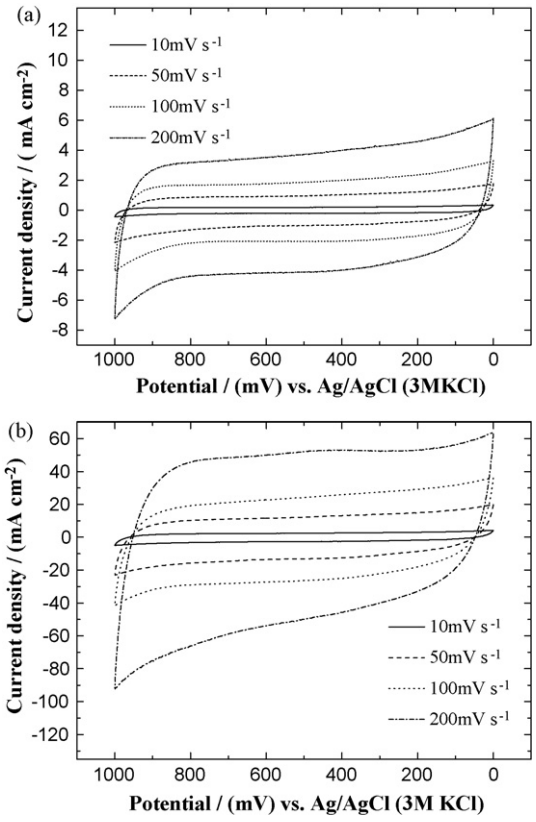

Fig. 3. Cyclic voltammograms measured at different scan rates for the SnO_x coatings grown at 0.2 C cm^{-2} (a), and 2.0 C cm^{-2} (b) in 0.5 M KCl solution, respectively.

In order to inspect the capacitive characteristics of the deposited SnO_x coatings, cyclic voltammograms were recorded at various scan rates in 0.5 M KCl electrolyte. Fig. 3 presents the CVs of the SnO_x coatings grown at 0.2 (see Fig. 3a), and 2.0 C cm^{-2} (see Fig. 3b) in 0.5 M KCl solution, respectively. These CVs show clearly the rectangular and symmetric current–potential characteristics of an ideal capacitive, except at potentials near the two limits of the potential window. In addition, even at a high potential scan rate of 200 mV s^{-1}, the CVs were still found to show a capacitive-like behavior, i.e., a rectangular-like shape. CVs were also recorded in the same electrolyte with bare graphite electrode, implying no capacitive behavior with negligible current response with respect to that shown in Fig. 3. The highly porous SnO_x coating may have a large surface area preferred for double-layer processes, but a large magnitude of current response in cyclic voltammetry cannot merely be attributed to the double-layer processes. More significantly, the voltammetric current response exhibits direct

proportionality to the applied potential scan rate, and the specific capacitance can consequently be calculated using the formula given below.

$$C_{CV} = \frac{i}{[(dE/dt)A]} = \frac{I}{(dE/dt)} \quad (3)$$

where i is the voltammetric current, dE/dt the potential scan rate, A the surface area of the graphite electrode, and I the voltammetric current density. Accordingly, a specific capacitance (in milli-farad per square centimeter, C_a) of as high as 255 mF cm^{-2} was achieved for the SnO_x coating grown at 2.0 C cm^{-2}. For a SnO_x coating deposited at a charge of 0.2 C cm^{-2}, a maximum specific capacitance (in farad per gram, C_m) of 298 and 125 F g^{-1} was obtained from CVs at a scan rate of 10, and 200 mV s^{-1}, respectively. For the coating grown at 2.0 C cm^{-2}, 206 F g^{-1} and 92 F g^{-1} are, however, reached.

The charge–discharge behaviors of the SnO_x coatings were also examined by chronopotentiometry between 0 and 1 V in 0.5 M KCl solution. The specific capacitance can, thus, be evaluated from the following equation,

$$C_{CP} = \frac{i}{|(dE/dt)A|} = \frac{i}{[(\Delta E/\Delta t)A]} \quad (4)$$

where i is the charge–discharge current applied, (dE/dt) the slope of the charge–discharge plot of the CP curves, and A the surface area of the graphite electrode.

Fig. 4 presents the charge–discharge plots of the SnO_x coatings at a current density of 7.08 mA cm^{-2} (a current of 2.0 mA was applied), showing the symmetric and similar E–t curves.

Depositions at more charge were conducted, and the as-grown SnO_x coatings were measured via chronopotentiometry under the same conditions in order to examine the variation of specific capacitance on the SnO_x coating thickness. A serious problem was encountered with the thick coatings deposited at a charge above 4.5 C cm^{-2}. Extreme care had to be taken with such relatively thick coatings in order to prevent small pieces from peeling off the coating. As shown in Fig. 5a, the average specific capacitance (C_a) increases to a capacitance as high as 355 mF cm^{-2}. The data reported in Fig. 5a were derived from the chronopotentiometric measurements between 0 and 1 V at a current density

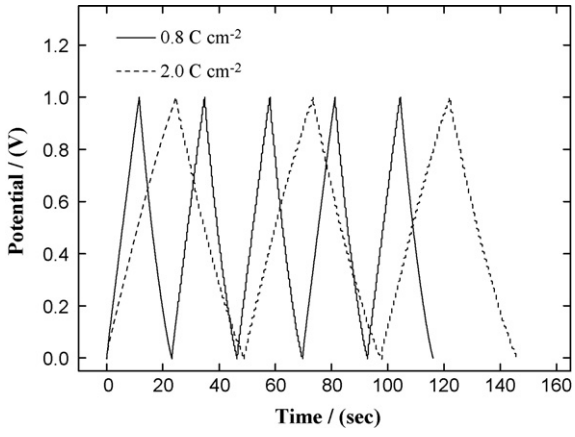

Fig. 4. The charge–discharge plots of the SnO_x coatings at a current density of 7.08 mA cm^{-2} (a current of 2.0 mA was applied).

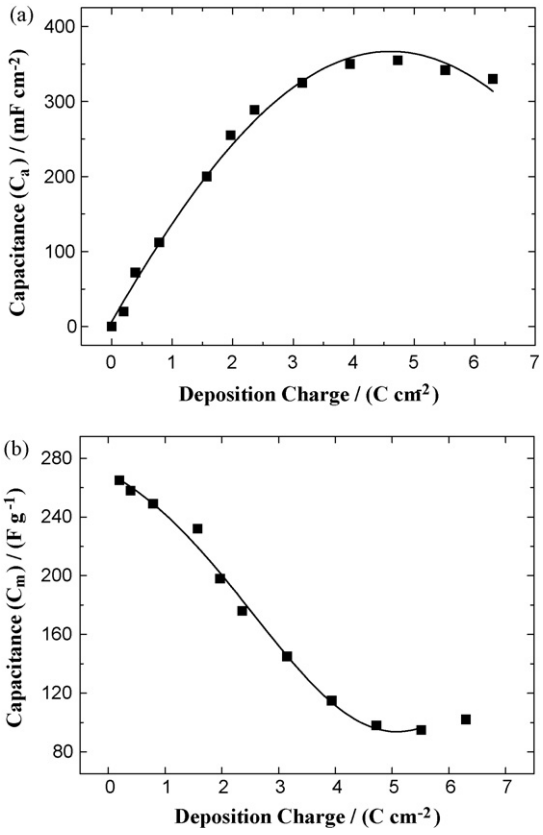

Fig. 5. Specific capacitance vs. deposition charge in 0.5 M KCl solution. Capacitance was measured from chronopotentiometry between 0 and 1 V at a current density of 0.885 mA cm^{-2} (a current of 0.25 mA was applied).

of 0.885 mA cm^{-2} (a current of 0.25 mA was applied). Most interestingly, the relationship of specific capacitance with the deposition charge exhibits linearity in the range of 4.5 C cm^{-2}, and there is a peak at around 5 C cm^{-2}. This finding is similar to that with highly porous amorphous MnO_2 coatings, reported by Broughton and Brett [40]. In addition, the author clarified some of the disadvantages of simply using thicker films to improve C_a since a trend of getting C_m decreased is distinct. Although there is a maximum value of C_a, the value of C_m is always decreasing to near 100 F g^{-1}, correspondingly. The as-grown SnO_x coatings most likely go with the similar characteristics. One may see clearly from Fig. 5b that a decrease in C_m becomes relatively significant with the increase of the thickness of the coatings, with a result of that C_m gets lower from 265 to around 95 F g^{-1} corresponding to the maximum of C_a.

To explain the results, we have to appeal to understanding the charge storage mechanism of SnO_x coatings in neutral aqueous electrolyte solutions. One might assume that SnO_x has a similar charge storage mechanism to MnO_2. Two main mechanisms were proposed to explain the MnO_2 charge storage. The first suggests the intercalation of protons (H^+) or alkali metal cations in the bulk of the material upon reduction followed by de-intercalation upon oxidation [13]. The second is based on the surface adsorption of alkali metal cations on MnO_2 [41]. Recently, combination of the two explanations is made to get a better understanding of the charge storage mechanism

in MnO_2 electrodes [42]. Most importantly, protons and alkali metal cations from the electrolyte are confirmed to be involved simultaneously in the charge storage process of MnO_2 thin film electrodes, and alkali metal cations are anticipated for charge compensation. As a consequence, alkali metal cations play an important role in the charge–discharge electrochemistry of SnO_x coating. A mechanism based on the surface adsorption of electrolyte cations (C^+) such as K^+ on SnO_x could be suggested as follows,

$$(SnO_x)_{surface} + C^+ + e = (SnO_x{}^-C^+)_{surface} \quad (5)$$

and simultaneously, the intercalation of H^+ or alkali metal cations (C^+) in the bulk of the coating upon reduction followed by de-intercalation upon oxidation.

$$SnO_x + H^+ + e = SnO_xH \quad (6)$$

$$SnO_x + C^+ + e = SnO_xC \quad (7)$$

Reasonably high conductivity of SnO_x and the formation of nanostructured and microporous material could be attributed to more electrolyte cations adsorbed on the large surface, and preferred the high values of capacitance found in the present study. It is in agreement with the observation of SEM images, from which we can conclude that the accessible surface for electrolyte cation adsorption is presumably getting larger initially, and smaller at the peak. Fig. 6 shows the relationship between specific capacitance and charge–discharge current density applied. It is believed that the redox reactions occurring in SnO_x coated electrode involve intercalation of protons and alkali metal cations into the coating. Accordingly, the specific capacitance appears decreasing with increase in the applied charge–discharge current density.

Cyclic charge–discharge tests between 0 and 1 V (versus Ag/AgCl) were conducted with the SnO_x coatings grown at different deposition charge since the long-term operation stability of an electro-active material is of great importance. Fig. 7 presents the variation of C_a as a function of cycle number. A decrease of about 10.0 %, 15% and 18% of C_a was observed after 1000 cycles for the coatings grown at 0.8, 2.0 and 4.0 C cm^{-2}, respectively. Capacitance was measured from chronopotentiometry between 0 and 1 V at a current density of 1.77 mA cm^{-2} (a current of 0.5 mA was applied). For the above three electrodes, there is an eminent decrease for the first 100 cycles and the value of C_a remains almost unchanged afterwards. A decrease of around 3.0% was observed between 100 and 1000 cycles, which is much comparable to that reported by Miura and Prasad [33] for potentiodynamically deposited SnO_2 films, and that achieved for MnO_2 coatings [14].

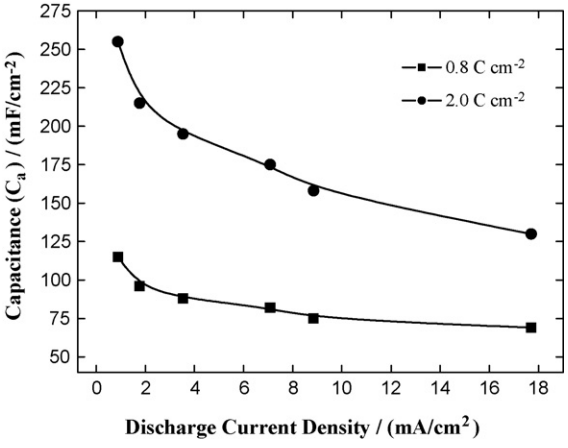

Fig. 6. Relationship between specific capacitance and charge–discharge current density applied.

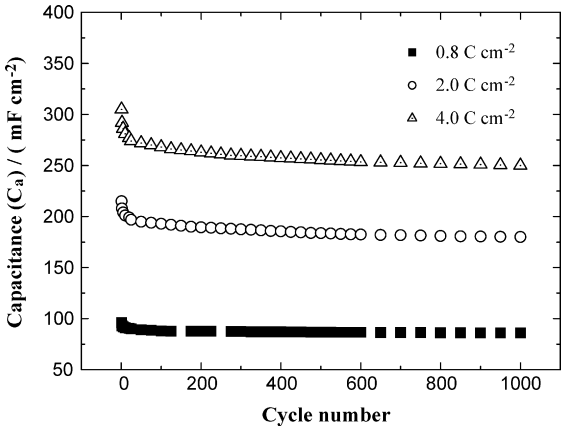

Fig. 7. Cycle-life of SnO_x coatings grown at different deposition charge. Capacitance was measured from chronopotentiometry between 0 and 1 V at a current density of 1.77 mA cm^{-2} (a current of 0.5 mA was applied).

4. Conclusions

Amorphous tin oxide (SnO_x) was cathodically deposited onto graphite electrode in a bath containing 0.1 M stannous chloride ($SnCl_2$), 0.5 M sodium nitrate ($NaNO_3$), and 0.4 M nitric acid (HNO_3) in an aqueous solution of 50% (v/v) ethanol. The SnO_x coatings grown on graphite were characterized as typical capacitive behaviors by cyclic voltametry (CV), chronopotentiometric (CP) in 0.5 M KCl. Dependence of deposition conditions on the capacitive properties of SnO_x coatings was demonstrated. The relationship of specific capacitance with the deposition charge exhibits linearity in the range of 4.5 C cm^{-2}, and there is a maximum as high as 355 mF cm^{-2} with the coating deposited at around 5 C cm^{-2}. A decrease in C_m, however, becomes relatively significant with the increase of the thickness of the coatings. It was demonstrated that C_m gets lower from 265 F g^{-1} to around 95 F g^{-1} corresponding to the maximum of C_a. The as-grown SnO_x coatings show long cycle-life and good stability.

Acknowledgement

M. Wu would like to give thanks to the financial support from the Sichuan Youth Science and Technology Foundation of China.

References

[1] J.P. Zheng, P.J. Cygan, T.R. Jow, J. Electrochem. Soc. 142 (1995) 2699.
[2] T. Liu, W.G. Pell, B.E. Conway, Electrochim. Acta 42 (1997) 3541.

[3] A.A.F. Grupioni, E. Arashiro, T.A.F. Lassali, Electrochim. Acta 48 (2002) 407.
[4] K.C. Liu, M.A. Anderson, J. Electrochem. Soc. 143 (1996) 124.
[5] V. Srinivasan, J.W. Weidner, J. Electrochem. Soc. 144 (1997) L210.
[6] V. Srinivasan, J.W. Weidner, J. Electrochem. Soc. 147 (2000) 880.
[7] A.A.F. Grupioni, T.A.F. Lassali, J. Electrochem. Soc. 148 (2001) A1015.
[8] K.W. Nam, W.S. Yoon, K.B. Kim, Electrochim. Acta 47 (2002) 3201.
[9] E.E. Kalu, T.T. Nwoga, V. Srinivasan, J.W. Weidner, J. Power Sources 92 (2001) 163.
[10] V. Srinivasan, J.W. Weidner, J. Power Sources 108 (2002) 15.
[11] H.K. Kim, T.Y. Seong, J.H. Lim, W.L. Cho, Y.S. Yoon, J. Power Sources 102 (2001) 167.
[12] C. Lin, J.A. Ritter, B.N. Popov, J. Electrochem. Soc. 145 (1998) 4097.
[13] S.-C. Pang, M.A. Anderson, T.W. Chapman, J. Electrochem. Soc. 147 (2000) 444.
[14] R.N. Reddy, R.G. Reddy, J. Power Sources 124 (2003) 330.
[15] M. Wu, G.A. Snook, G.Z. Chen, D.J. Fray, Electrochem. Commun. 6 (2004) 499.
[16] W. Dong, J. Sakamoto, B. Dunn, J. Sol–Gel Sci. Techn. 26 (2003) 641.
[17] W. Dong, J.S. Sakamoto, B. Dunn, Sci. Tech. Adv. Mater. 4 (2003) 3.
[18] S.-Y. Wang, N.-L. Wu, J. Appl. Electrochem. 33 (2003) 345.
[19] S.-Y. Wang, K.-C. Ho, S.-L. Kuo, N.-L. Wu, J. Electrochem. Soc. 153 (2006) A75.
[20] C.Z. Deng, R.A.J. Pynenburg, K.C. Tsai, J. Electrochem. Soc. 145 (1998) L61.
[21] T.C. Liu, W.G. Pell, B.E. Conway, S.L. Roberson, J. Electrochem. Soc. 145 (1998) 1882.
[22] M. Kalaji, P.J. Murphy, G.O. Williama, Synth. Met. 102 (1999) 1360.
[23] A. Laforgue, P. Simon, C. Sarrazin, J.-F. Fauvarque, J. Power Sources 80 (1999) 142.
[24] K.A. Noh, D.-W. Kim, C.-S. Jin, K.-H. Shin, J.H. Kim, J.M. Ko, J. Power Sources 124 (2003) 593.
[25] G.Z. Chen, M.S.P. Shaffer, D. Coleby, G. Dixon, W. Zhou, D.J. Fray, A.H. Windle, Adv. Mater. 12 (2000) 522.
[26] M. Hughes, G.Z. Chen, M.S.P. Shaffer, D.J. Fray, A.H. Windle, Chem. Mater. 14 (2002) 1610.
[27] M. Wu, G.A. Snook, V. Gupta, M.S.P. Shaffer, D.J. Fray, G.Z. Chen, J. Mater. Chem. 15 (2005) 2297.
[28] T. Brousse, S.M. Lee, L. Pasquereau, D. Defives, D.M. Schleich, Solid State Ionics 51–56 (1998) 113.
[29] N.L. Wu, Mater. Chem. Phys. 75 (2002) 6.
[30] S.L. Kuo, N.L. Wu, Electrochem. Solid State Lett. 6 (2003) A85.
[31] H.-K. Kim, S.-H. Choi, Y.S. Yoon, S.-Y. Chang, Y.-W. Ok, T.-Y. Seong, Thin Solid Films 475 (2005) 54.
[32] M. Jayalakshmi, N. Venugopal, K.P. Raja, M.M. Rao, J. Power Sources 158 (2006) 1538.
[33] K.R. Prasad, N. Miura, Electrochem. Commun. 6 (2004) 849.
[34] M.M. Rao, M. Jayalaksmi, B.R. Reddy, S.S. Madhavendra, M.L. Kantam, Chem. Lett. 34 (5) (2005) 712.
[35] S.T. Chang, I.C. Leu, M.H. Hon, J. Cryst. Growth 273 (2004) 195.
[36] C.C. Streinz, A.P. Hartman, S. Motupally, J.W. Weidner, J. Electrochem. Soc. 142 (1995) 1084.
[37] C.C. Streinz, S. Motupally, J.W. Weidner, J. Electrochem. Soc. 142 (1995) 4051.
[38] M. Wu, J. Gao, S. Zhang, A. Chen, J. Power Sources 159 (2006) 365.
[39] M. Drogowska, H. Menard, J. Appl. Electrochem. 21 (1991) 84.
[40] J.N. Broughton, M.J. Brett, Electrochim. Acta 50 (2005) 4814.
[41] H.Y. Lee, J.B. Goodenough, J. Solid State Chem. 144 (1999) 220.
[42] M. Toupin, T. Brousse, D. Belanger, Chem. Mater. 16 (2004) 3184.